Novel and Sustainable Colorants Developed via Incorporating Azo Chromophores into Dopamine Molecules

Suju Fan, Yintung Lam, Liang He, and John H. Xin*

Read Online

ACCESS | Metrics & More | Article Recommendations | SI Supporting Information

ABSTRACT: Inspired by the application of dopamine as an "anchor" and UV absorber, novel sustainable colorants with biscatecholic structure were synthesized through a simple incorporation of simple azo chromophores with dopamine. Their structures were confirmed using MS and NMR analyses, and their application on textile materials was investigated. Compared to the simple azo chromophores with almost no coloring ability on fabrics, the biscatecholic colorants could color different fabrics effectively, mainly through self-polymerization only in the presence of a trace amount of organic base at room temperature, which is environmentally friendly in terms of saving resources and alleviating chemical pollution. Meanwhile, the UV resistance of colored fabrics was enhanced significantly, showing the advantage of protecting wearers from UV damage.
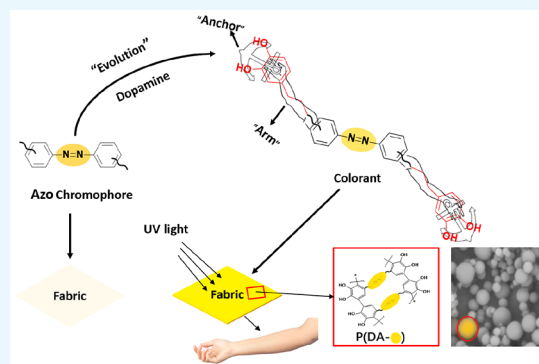
1. INTRODUCTION

3,4-Dihydroxy-L-phenylalanine (DOPA) is an amino acid found in adhesive proteins secreted by marine mussels, which is one organism in nature and exhibits unique adhesion on rocks.[1−3] It is believed that DOPA plays an important role in the adhesion mechanism of marine mussel through cross-linking and different physicochemical interactions.[4−6] In much research, dopamine is frequently used as an alternative for DOPA to mimic adhesive protein because of its similar structure to DOPA and more wide distribution.[7] Dopamine could generate surface-adherent films on diverse substrates through self-polymerization, but the mechanism is complex and still elusive. Many researchers have suggested that it is attributed to the oxidation of catechol under alkaline conditions.[6,8−11] Based on the adhesive property, dopamine is widely used as a sustainable coating material through codeposition with other materials including inorganic materials, polymers, and nanoparticles.[10,12−15]

With the benefits of having catechol and amine groups, dopamine could be used as the starting points for covalent modification with molecules, and therefore it is often used to conjugate with other molecules or material surfaces to achieve functional applications, such as bioadhesives or magnetic nanoparticles.[4,16−22] However, few studies have been focused on its application on coloration. Furthermore, dopamine has an obvious absorption peak at ca. 280 nm, and its UV absorbance can be increased significantly via the self-polymerization into polydopamine (pDa), which is also known as a major pigment of natural melanin.[9,23,24] Hence, dopamine−melanin has already been used as an effective UV absorber to enhance the UV-shielding performance of nanoparticles and films.[25,26] The fabric treated with dopamine has been reported to show better UV resistance.[27]

Therefore, the effective utilization of functional properties of dopamine on textiles will be a useful and potential strategy. In our previous studies, dopamine was applied to color various natural and synthetic textile materials through different methods including polydopamine-assisted dyeing and chemical modification, and all the studies showed positive results.[28−30] To continue our interest, herein we bonded covalently simple azo chromophores with dopamine molecules, successfully synthesizing a kind of novel and sustainable colorant. In the structure of the colorants, the azo groups were used as the chromophores and catechols on dopamine as the anchoring points. Compared with the dyes used in previous studies, the azo molecules selected in this work are just simple and common models containing chromophores, with inferior coloring ability on materials. The synthesized biscatecholic colorants demonstrated enhanced coloring performance and good UV-shielding properties. They could be regarded as the products of "evolution" by growing the arms holding anchors (as shown in Figure 1). This study provides a more comprehensive extension for the application of dopamine in textile fields.
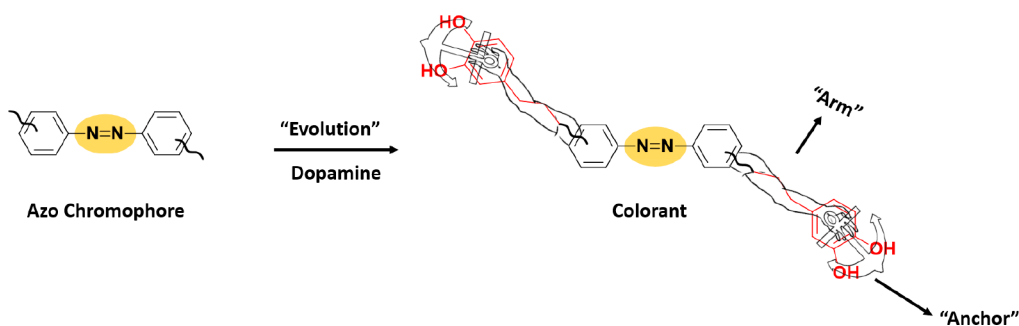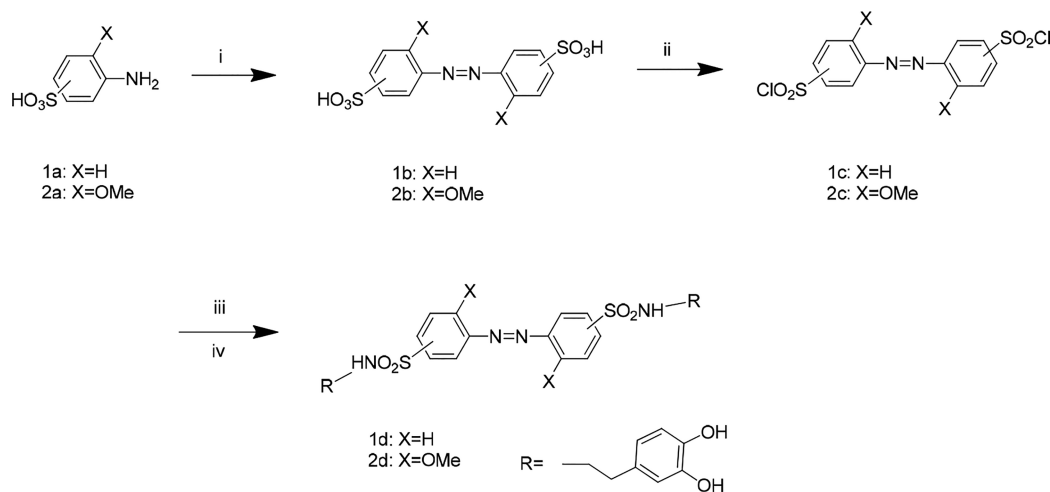
Figure 1. Illustration of the evolutionary process from an azo chromophore to a colorant.

Scheme 1. Synthesis Route and Chemical Structures of the Biscatecholic Colorants[a]

Colorants	Structure	Yield %
1d		49.5
2d		45.2

[a](i) NaClO/ice bath; (ii) (ClCO)$_2$/reflux; (iii) TBDMS-dopamine/K$_2$CO$_3$; (iv) TBAF/THF.

2. EXPERIMENTAL SECTION

2.1. Materials and Instruments. Aniline-4-sulfonic acid, 2-methoxyaniline-5-sulfonic acid, sodium hypochlorite solution with 6–14% active chlorine and 98% oxalyl chloride, 1.0 M tetrabutylammonium fluoride solution in THF, 4-dimethylaminopyridine (DMAP), and other reagent-grade chemicals were purchased from Shenzhen Dieckmann Technology Co., Ltd. and used without further purification.

High-resolution mass spectra were obtained on a Waters mass spectrometer. Nuclear magnetic resonance (NMR) spectra were recorded on a Jeol ECZ500R (500 MHz)

spectrophotometer. The absorption spectra were recorded on a UH5300 UV–vis spectrophotometer.

Colorimetric analyses of the fabrics were conducted using a Datacolor 650 spectrophotometer, and the results were recorded in the form of CIE, L^*, a^*, and b^* color space, and K/S values. Wash fastness, crocking fastness, and light fastness were assessed using the same method used in a previous report.[29]

The surface morphology of fibers was characterized using a Hitachi TM3000 Benchtop Scanning Electron Microscope (SEM) from Japan, and cross-section images were investigated

Scheme 2. Comparison of the Diazotization Coupling Reaction and Oxidization Coupling Reaction

(a) Diazotization coupling reaction

(b) Oxidization coupling reaction
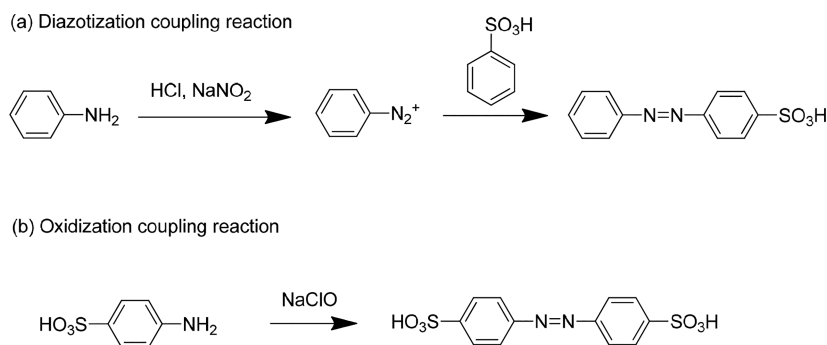
on an optical microscope: Nikon Optiphot-POL from Germany; UV−vis transmittance spectra and the ultraviolet protection factor (UPF) of colored fabrics were measured by a Varian Cary 300 UV−visible spectrophotometer.

2.2. Synthesis of Biscatechol Azobenzene Compounds. The synthesis route of biscatecholic colorants is shown in Scheme 1, and the preparation of sample **1d** is described in detail.

2.2.1. Synthesis of Azobenzene-4,4′-disulfonic Acid (1b). **1a**, aniline-4-sulfonic acid (0.35 g, 2 mmol), and anhydrous sodium carbonate (0.42 g, 4 mmol) were added to 20 mL of water under stirring. The resultant solution was cooled in an ice-salt bath, and 25 mL of sodium hypochlorite solution with about 6−14% activated chlorine was dropwise added. The mixture was further stirred for 3 h in the bath. Then, the solution was neutralized with diluted hydrogen chloride to pH 7.0, and the precipitate was collected by filtration. After washing with DI water and drying, the target product was obtained as orange solids. ^{1}H NMR (D$_2$O): δ 7.85−7.87 (d, 4H, ArH), 7.82−7.83 (d, 4H, ArH). HRMS (TOF, ES$^−$): m/z = 340.9735 (M − H) $^−$, calcd for C$_{12}$H$_{10}$N$_2$O$_6$S$_2$ 342.35.

2.2.2. Synthesis of Azobenzene-4,4′-disulfonyl Chloride (1c). **1b**, azobenzene-4,4′-disulfonic acid (0.34 g, 1 mmol), was added to 25 mL of oxalyl chloride and refluxed overnight. After the reaction, the solution was poured into 500 mL of ice water under stirring. Then, the mixture was filtrated and washed with ice water until the filtrate became neutral. The obtained solid was dried under a vacuum at room temperature. ^{1}H NMR (chloroform-*D*): δ 8.27−8.29 (d, 4H, ArH), 8.18−8.21 (d, 4H, ArH).

2.2.3. Synthesis of Catechol Derivative: TBDMS-dopamine. The solution of dopamine hydrochloride (0.95 g, 5 mmol) in 45 mL of dichloromethane was stirred in a water bath, and *tert*-butyldimethylsilyl chloride (2.26 g, 15 mmol) in 20 mL of dichloromethane was added dropwise to the solution over 15 min. The water bath was then replaced by an ice bath, and triethylamine (1.52 g, 15 mmol) was added to the mixture. After stirring in the bath for 1 h, the resultant reaction solution was further stirred for about 20 h at room temperature. Then, 50 mL of DI water was added into the solution under stirring, and the bottom layer was collected with a separation funnel. The collected solution was evaporated under vacuum to remove the solvent, and the target product was obtained as brown oil. HRMS (TOF, ES$^+$): m/z = 382.2596 (M + H)$^+$, calcd for C$_{20}$H$_{39}$NO$_2$Si$_2$ 381.70.

2.2.4. Synthesis of Biscatechol Colorant (1d). **1c**, azobenzene-4,4′-disulfonyl chloride (0.15 g, 0.4 mmol), TBDMS-dopamine (0.38 g, 1 mmol), anhydrous sodium carbonate (0.16 g, 1.5 mmol), and anhydrous sodium sulfate (0.21 g, 1.5 mmol) were added into 25 mL of anhydrous acetone. After stirring for 5 h at room temperature, the solvent was removed under vacuum, and the residue was added into 25 mL of tetrahydrofuran. An amount of 1 mL of TBAF solution was added, and the mixture was stirred for another 30 min at room temperature. Finally, the residue was obtained after removing THF and was purified by silica gel column chromatography using methanol/ethyl acetate/1,2-dichloro-ethane (1:1:5, v/v) as eluent to obtain **1d**. Yield: 49.5%. ^{1}H NMR (DMSO-d_6): δ 8.79 (s, 2H, OH), 8.72 (s, 2H, OH), 8.09 (d, 4H, ArH), 8.00 (d, 4H, ArH), 7.89 (t, 2H, ArH), 6.60 (d, 2H, ArH), 6.52 (s, 2H, NH), 6.38 (d, 2H, ArH), 2.93 (m, 4H, CH$_2$), 2.50 (m, 4H, CH$_2$). ^{13}C NMR (DMSO-d_6): δ 153.96, 145.48, 144.14, 143.49, 129.73, 128.47, 123.95, 119.73, 116.44, 115.33, 45.00, 35.24. HRMS (TOF, ES$^−$): m/z = 611.1278 [M − H]$^−$, calcd for C$_{28}$H$_{28}$N$_4$O$_8$S$_2$ 612.67.

2d was synthesized with similar procedures. Yield: 45.2%. ^{1}H NMR (DMSO-d_6): δ 8.75 (m, 4H, OH), 7.50 (d, 2H, ArH), 7.47 (d, 2H, ArH), 6.99 (d, 2H, ArH), 6.96 (s, 2H, ArH), 6.64 (d, 2H, ArH), 6.52 (s, 2H, ArH), 6.37 (t, 2H, NH), 3.72 (s, 6H, CH$_3$), 2.57 (t, 4H, CH$_2$), 2.43 (t, 4H, CH$_2$). ^{13}C NMR (DMSO-d_6): δ 151.22, 145.46, 144.10, 143.52, 132.13, 129.88, 128.25, 119.82, 117.15, 116.54, 115.94, 112.82, 56.60, 44.77, 35.04. HRMS (TOF, ES$^−$): m/z [M − H]$^−$, calcd for C$_{30}$H$_{32}$N$_4$O$_{10}$S$_2$ 672.73, found 671.1491.

2.3. Coloration. Textile fabrics were washed with 5 g/L of sodium dodecyl sulfate solution at 60 °C for 20 min to remove surface impurities and then washed with DI water and dried in air. Then, fabrics were immersed in 0.05% (w/v) colorant solution in methanol (liquor ratio 50:1) with and without 0.2 mg/mL of DMAP, respectively, at room temperature for 24 h and subsequently rinsed with water. After drying, the fabrics were washed with 0.5% detergent at 60 °C for 10 min to remove the unfastened colorant and then air-dried. For comparative purposes, both azo chromophores (**1b** and **2b**) and commercial dye acid yellow 11 (AY11) were used to color fabrics in water with and without 0.2 mg/mL of DMAP, respectively.

3. RESULTS AND DISCUSSION

3.1. Synthesis and Characterization. Azo compounds are usually synthesized through a diazotization coupling reaction, with asymmetric structures[31−34] (as shown in Scheme 2a). However, the novel colorants developed in this study are biscatecholic azobenzene compounds with a symmetric structure, and their precursors, the azo chromophores, are suitable to be synthesized via an oxidization−coupling reaction,[35−37] where aromatic amines can self-couple to form
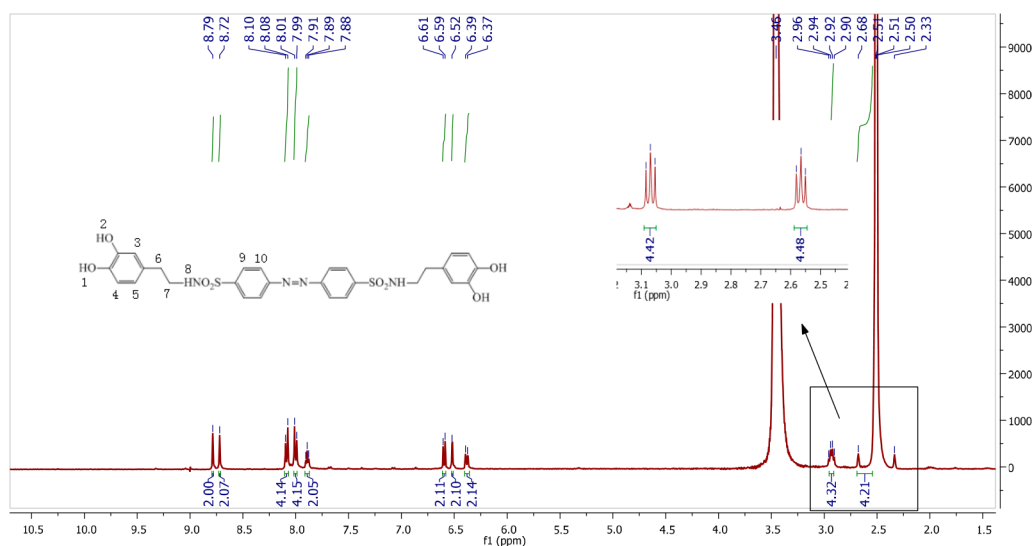
Figure 2. ^{1}H NMR spectrum of **1d** in DMSO-d_6. Inset: partial ^{1}H NMR spectrum in methanol-d_4.

azo bonds (as shown in Scheme 2b). Based on the symmetric structure, two dopamine molecules could be simply incorporated into the azo chromophore through a one-step reaction. For the oxidization−coupling reaction, air can be used as an oxidation agent in the presence of metal catalysts, such as Ag, Pt, Au, and Pd.[38−42] Comparably, sodium hypochlorite offers the advantages of low cost, easy availability, and proper oxidization ability.[37] Therefore, sodium hypochlorite was employed in this study. The obtained sulfonic acid of azo compounds can be easily converted to chlorosulfonyl derivatives through a chlorination process in the presence of chlorination reagents, such as chlorosulfonic acid, phosphorus oxychloride, and thionyl chloride.[43,44] In this work, oxalyl chloride was used as the chlorination reagent because of its mild reactivity and easy post-treatment involved.[45] In order to protect the catecholic groups of dopamine molecules during the synthesis process, *tert*-butyldimethylsilyl chloride was used since it has moderate stability and can easily be removed in the presence of TBAF under mild conditions at the final stage.[46−49]

3.2. Characterization of Biscatecholic Colorants. The structures of colorants **1d** and **2d** were deduced with the aid of MS and NMR data. One thing worth noting is that the peaks for H6 at ca. δ 2.50 ppm obviously interfered with the solvent residual peak, as shown in Figure 2 (^{1}HNMR spectrum in DMSO-d_6) for **1d**. Therefore, the peaks were further verified with methanol-d_4 as the solvent. It could be observed from the inset image in Figure 2 that two clear triplets with a correct ratio of the integral area confirmed the presence of H7 and H6. More spectra could be found in the Supporting Information.

3.3. UV−vis Absorption Spectra. The absorption spectra of three compounds **1d**, **2d**, and dopamine in methanol with the concentration of 0.01 mg/mL were shown in Figure 3. Compared to the absorption peak of dopamine at ca. 280 nm, the phenolic hydroxyl absorption appeared in the spectrum of the as-synthesized compounds, and the wavelengths of maximum absorbance (λ_{max}) of **1d** and **2d** were located at ca. 326 and 372 nm, respectively. Two compounds had the same chromophore of azobenzene, but the electron-donating methoxy group on **2d** contributed to the increase of electron cloud density, resulting in bathochromic shifts of λ_{max}. The
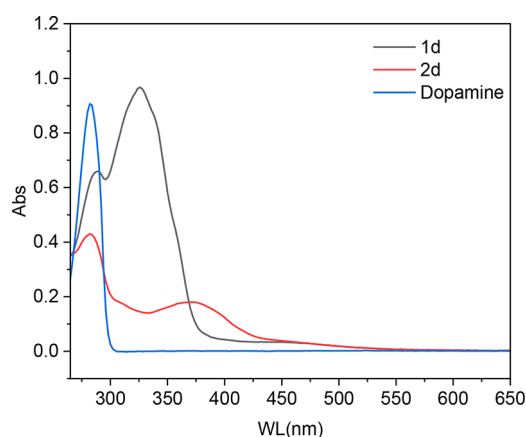

Figure 3. UV−vis spectra of **1d**, **2d**, and dopamine in methanol.

molar attenuation coefficients of **1d** and **2d** were shown in Table 1.

Table 1. Molar attenuation Coefficient (ε) of the Biscatecholic Colorants in Methanol

compounds	1d	2d
ε (L·mol^{-1}·cm^{-1})	5.91×10^4	1.33×10^4

The λ_{max} values of the biscatecholic colorants in different solvents were also studied. As listed in Table 2, the λ_{max} of these compounds was similar in polar and less polar solvents, which indicated that their absorptions showed no obvious dependence on solvent polarity.

3.4. Colorimetric Analysis. Fabrics colored with **1b**, **1d**, **2b**, and **2d** colorants in solvent with and without the presence

Table 2. λ_{max} of the Biscatecholic Colorants in Different Solvents^a

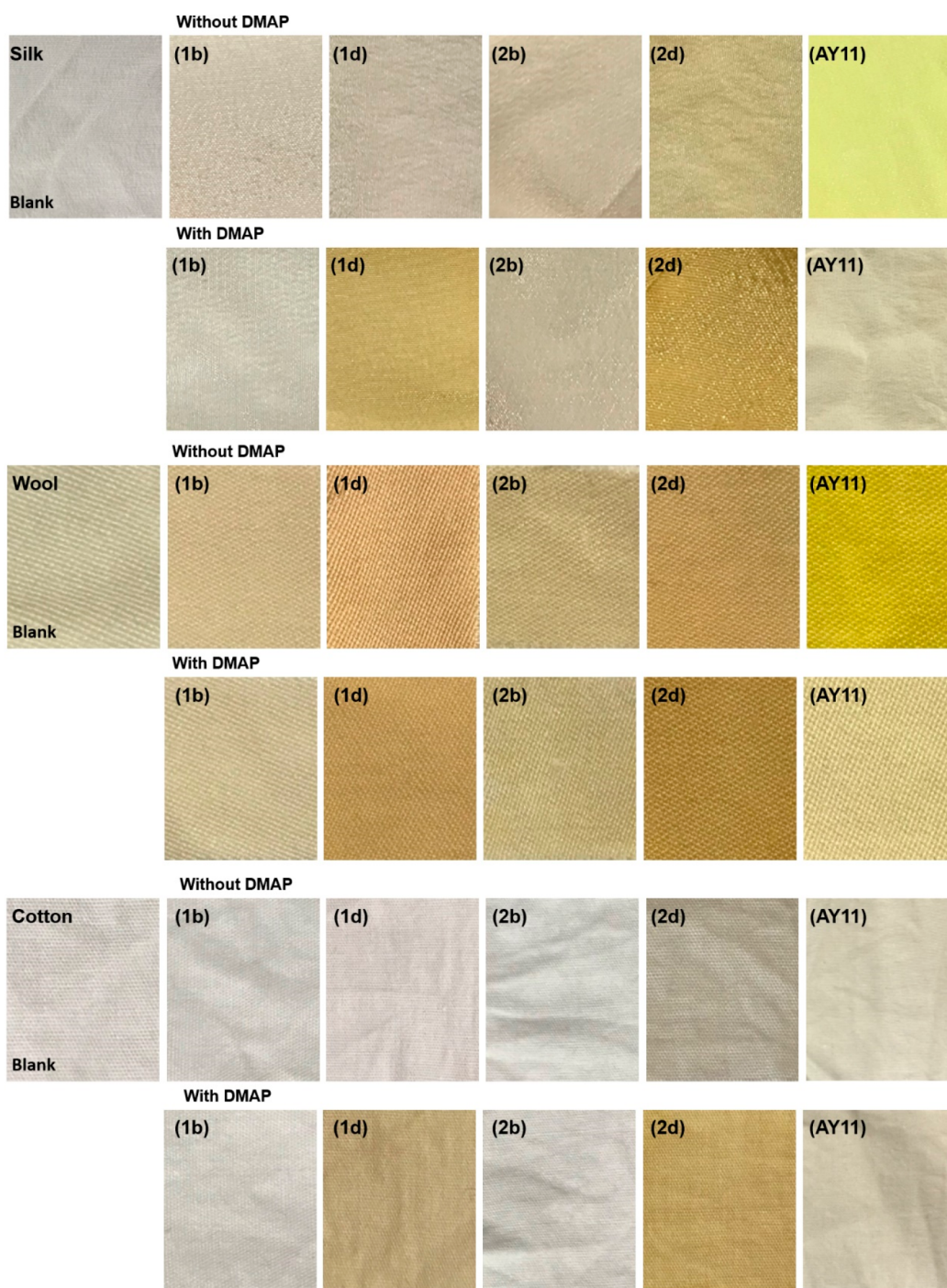| compounds	methanol/nm	ethanol/nm	DMF/nm	acetone/nm
1d	326	325	330	332
2d	372	370	376	374

^{a}DMF: *N,N*-dimethylformamide.

Figure 4. Photographic images of the coloration results of common textile materials. **1b**, **2b**, and AY11 colored fabrics in water; **1d** and **2d** colored fabrics in methanol; with and without organic base: DMAP (4-dimethylaminopyridine).

of DMAP (organic base) were evaluated by colorimetric analysis. As shown in Figure 4, the appearance of fabrics colored by **1d** and **2d** without DMAP is deeper than that of **1b** and **2b**, but the enhanced effects were not distinct, especially on silk and cotton. Compared to commercial dye AY11, the coloration effect of as-synthesized colorants on textile materials also had no obvious advantage. However, the coloring ability of **1d** and **2d** was enhanced significantly with the presence of DMAP, and all colored fabrics showed more distinct color appearance than that of **1b** and **2b** as well as acid yellow 11.

As the simple models contained only chromophore, **1b** and **2b** could hardly color fabrics either with or without DMAP. One of the possible reasons was that these molecules were small, making them difficult to be trapped between fibers. More importantly, their interaction with fabric might only involve weak Van der Waals forces. These could be attributed to their little coloring ability on fabrics and make them useless as colorants though they have a chromophoric group.

Without DMAP, the coloring ability of **1d** and **2d** was mainly attributed to hydrogen bonding between their hydroxyl groups and the hydroxyl and amino groups on fibers. Different

from other commercial dyes, as-synthesized compounds have a longer molecular chain and special symmetrical structure; hence the intramolecular hydrogen bonding could be easily formed. This would cause the decrease in the interaction between hydroxyl groups on colorants and fabrics, leading to poor coloring performance. The existence of intramolecular hydrogen bonds could be revealed from the FTIR spectra of the solution of as-synthesized compounds in Figure 5, of which
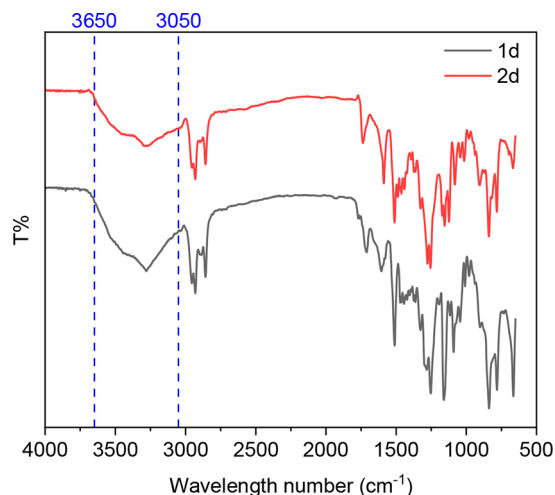

Figure 5. FTIR spectra of a solution of **1d** and **2d** in methanol.

there was a wide and strong peak between 3650 and 3050 cm^{-1}. However, these fabrics could be colored with **1d** and **2d** effectively in the presence of DMAP. Researchers have shown that organic base could catalyze the formation of a polydopamine (pDA) coating on substrates in aqueous conditions,[50−53] and the presence of organic base is important for the deprotonation of dopamine and also the subsequent oxidative polymerization.[54] In this study, organic base (DMAP; pK_b is about 4.4 under the standard state) also played an important role in the coloration of **1d** and **2d** on fabrics, improving their coloring ability significantly. We assumed that in the presence of DMAP the polymerization of **1d** and **2d** could also take place, and then the formed polymers coated the fabrics, which is similar to the formation principle of

dopamine-based adhesive coatings on various materials. This explanation could be supported by the coating of a metal substrate with as-synthesized colorants at a higher concentration (as shown in Figure 6a−d). After collection and evaluation with a scanning electron microscope, spherical morphologies of the deposited particles formed through self-polymerization of colorant molecules were observed clearly (as shown in Figure 6e−g). Compared to the particles formed by dopamine, the diameter of particles formed by as-synthesized colorants was larger. This could be reasonably explained by the size expansion of combining a large azo chromophore molecule with two dopamine molecules. It is worth mentioning that both the surface and interior part of the fibers could be "coated" because the molecules of **1d** and **2d** were small and could easily enter the inside of the fibers before polymerization. The colored cross section of fibers could be used to support the proposed idea (as shown in Figure 7). Compared with the bases used in other studies such as piperidine and trimethylamine, DMAP has a higher nucleophilicity which is beneficial for the polymerization[54−56] and slighter small for application. The chemical interactions (Michael addition or Schiff base reaction) suggested in many studies[6,16,57−59] were also likely involved in the process of coloring (Figure S1). The addition of DMAP had an adverse impact on the coloring performance of AY11, which had no functional catechol group.

The surface morphology of colored fibers was also investigated, as shown in Figure 8. The surface morphologies of colored silk and wool were rougher than that of blank fabrics, while the roughness of cotton before and after coloration had a negligible difference. This result was probably attributed to the better resistance of cotton fabric to alkali than that of protein fabrics (silk and wool). On different fiber surfaces, microscaled particles originating from the colorants could be observed to various extents. Microscaled particles on wool were the most obvious, while those on cotton were the least obvious. The result was in line with the K/S value of three colored fabrics found, where the wool had the highest value and the cotton had the lowest value (as shown in Table 3). The possible cause for this was that wool had a tighter and rougher structure than silk and cotton, contributing to the trapping and aggregation of particles. In addition, wool had more thiol groups which were beneficial for chemical
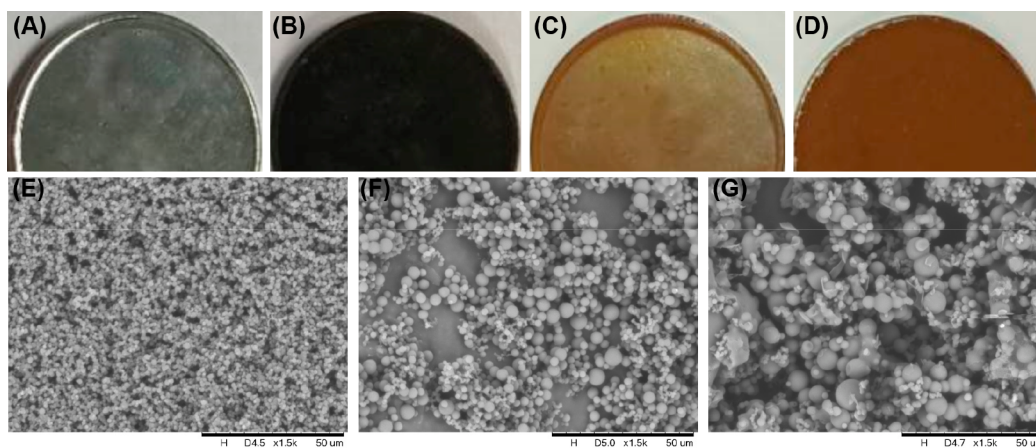

Figure 6. Photographic images of a metal substrate coated by 5 mg/mL of dopamine and biscatecholic colorants, respectively, in methanol with 5 mg/mL of DMAP: (A) blank metal substrate, (B) dopamine, (C) **1d**, (D) **2d**. The SEM images of polymerized particles: (E) polydopamine (pDa), (F) poly-**1d**, and (G) poly-**2d**.
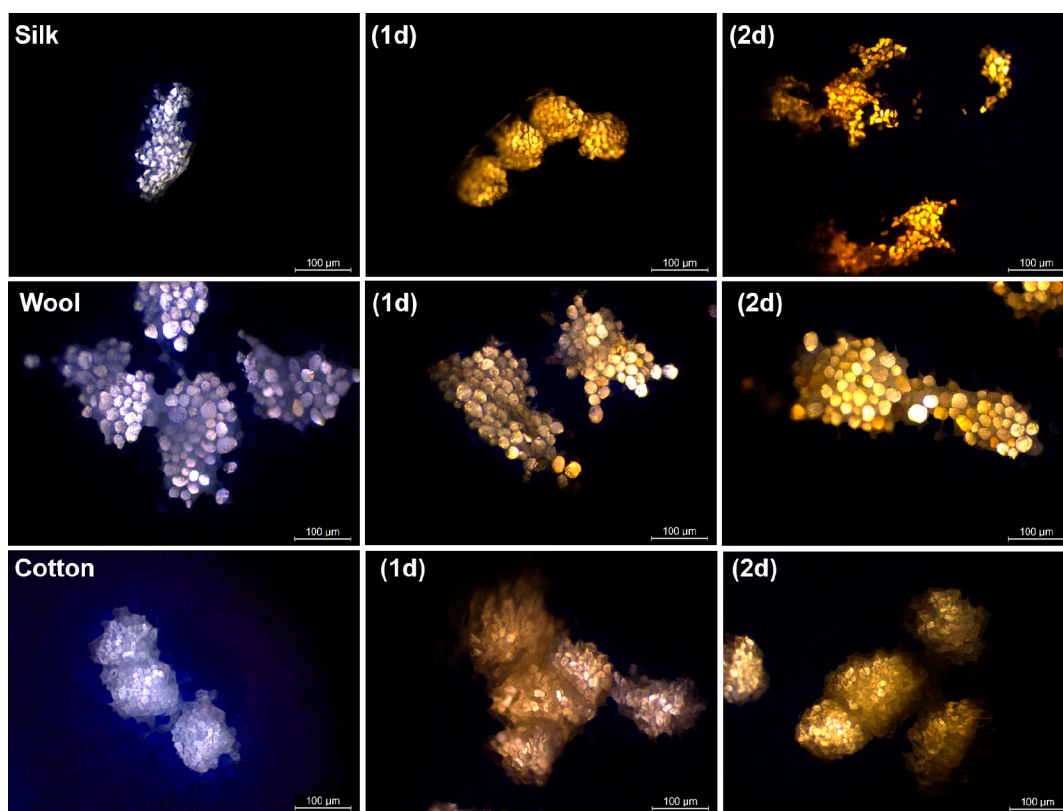
Figure 7. Microscopic images of the cross-section view of fibers before (far left) and after coloration with **1d** and **2d** with DMAP (blue fibers as background).
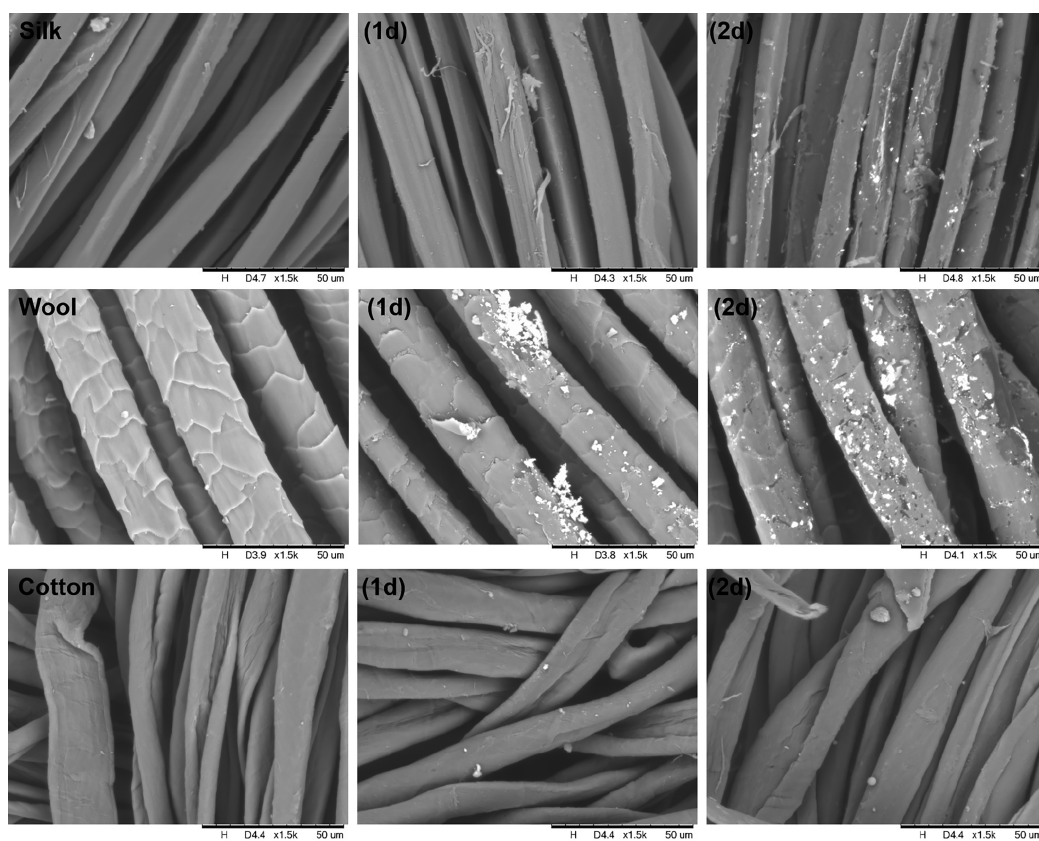

Figure 8. Surface morphology of fabrics before (far left) and after coloration with **1d** and **2d** with DMAP.

Table 3. Colorimetric Analysis and Fastness of the Colored Fabrics (1d and 2d with DMAP and AY11 without DMAP)

| fabrics	colorant	L^*	a^*	b^*	K/S	color change	wool	acrylic	polyester	nylon	cotton	acetate	dry	wet	light fastness
									staining				crocking fastness		
						wash fastness									
silk	blank	90.47	1.44	2.9	--	--	--	--	--	--	--	--	--	--	--
	1d	78.91	6.69	27.83	1.44	4	4−5	4−5	4−5	4−5	4−5	4−5	4−5	4	2−3
	2d	69.54	6.22	33.06	5.19	3−4	4−5	4−5	4−5	4−5	4−5	4−5	3−4	3	3
	AY11	87.41	4.92	46.73	2.51	1	3	4−5	4−5	3−4	4	4	4−5	4	3−4
wool	blank	87.42	3.02	0.75	--	--	--	--	--	--	--	--	--	--	--
	1d	73.9	7.19	18.88	3.38	3−4	4−5	4−5	4−5	4−5	3−4	4−5	4	4	2−3
	2d	71.4	5.61	23.7	5.47	3−4	4−5	4−5	4−5	4−5	3	4−5	3−4	3−4	3
	AY11	81.85	1.39	58.3	9.35	1	3	4−5	4−5	3−4	2−3	3−4	4−5	4−5	3−4
cotton	blank	95.25	3.63	11.78	--	--	--	--	--	--	--	--	--	--	--
	1d	79.76	3.78	13.23	0.73	4−5	4−5	4−5	4−5	4−5	4−5	4−5	4	4	2
	2d	80.12	2.95	23.77	1.79	3−4	4−5	4−5	4−5	4−5	4−5	4−5	4−5	3−4	3
	AY11	93.2	0.39	7.7	0.06	--	--	--	--	--	--	--	--	--	--
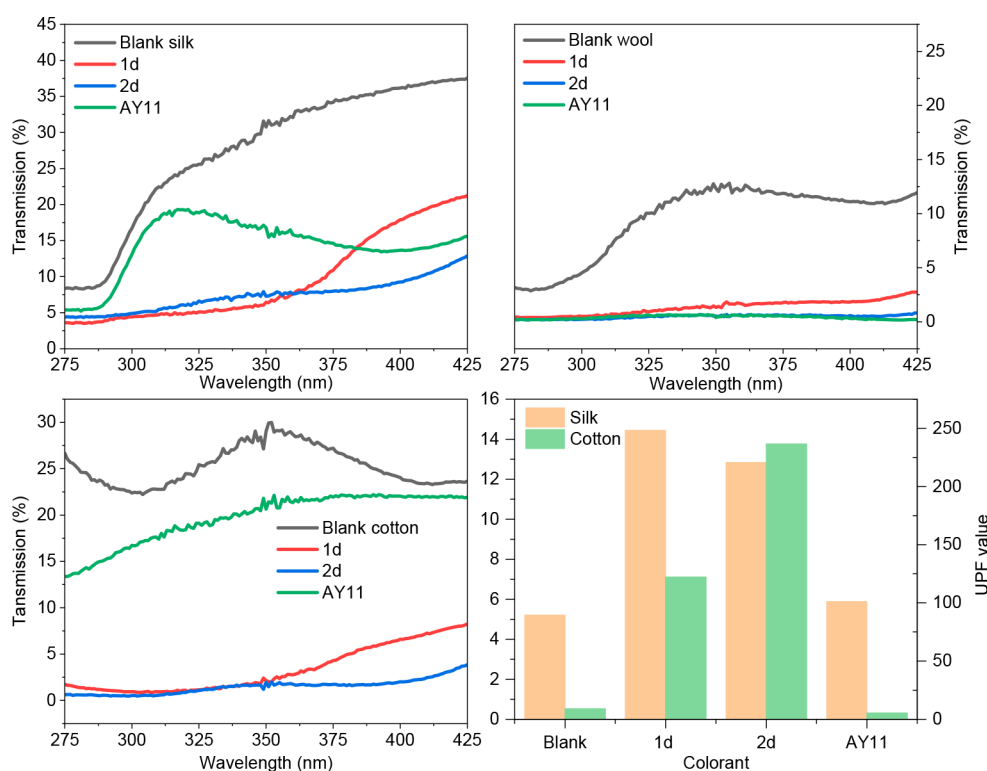
Figure 9. Transmittance spectra of colored fabrics with **1d**, **2d**, and AY11 and the UPF values of cotton and silk.

interactions between the wool fabric and the as-synthesized colorants. By contrast, the cotton fabric had a smoother surface, and it also had no effective functional groups supporting chemical interactions; therefore, the number of particles on its surface was fewer.

From the result of colorimetric analyses, as shown in Table 3, the color depth (K/S value) of fabrics colored with the as-synthesized colorants with DMAP was better than that without DMAP. The crocking fastness of fabrics colored with **2d** was poorer than that of **1d**, which was probably because **2d** had a bigger molecular volume and lower planarity, weakening the adhesive force between the polymers and the fibers.

3.5. UV Absorber. The transmittance spectra of the fabrics colored with **1d** and **2d** in the presence of DMAP were investigated. As shown in Figure 9, the UV transmittance of

the silk and cotton colored with **1d** and **2d** was reduced significantly, when compared to the spectra of blank fabrics. They also had lower transmittance than the fabrics colored with commercial AY11. Accordingly, their UPF values showed an obvious increase. This meant that their ability to protect wearers from UV damage was improved. This result would be positive and significant because silk and cotton are used frequently in summer outfits, but the UV protection property of these blank fabrics is generally insufficient. For wool fabric, the employment of as-synthesized colorants could also reduce its UV transmittance, and this reduction was relatively less distinct than that of silk and cotton because of its tighter fabric construction. Also, owing to this special structure, even for blank wool, its UV protection is good; therefore, its UPF increase made little sense, and there is no discussion about

that. Nevertheless, the results proved that **1d** and **2d** could endow textile materials with UV-shielding functionalities.

4. CONCLUSIONS

Two novel biscatecholic compounds were synthesized, which demonstrated how simple azo chromophores with little coloring ability "evolved" into effective colorants. Compared to some common commercial dyes, the novel colorants could color fabrics easily and effectively at room temperature without any chemical auxiliaries. The employment of them would greatly reduce energy and water consumption as well as reduce chemical pollution, which is environmentally friendly. Meanwhile, the fabrics colored with these compounds had an enhancement in terms of UV shielding effect and showed a significant increase in UV protection, an issue people often care about. Furthermore, by virtue of the obvious adhesive features, the colorants have a promising application on other materials such as synthetic substrates or glasses.

■ ASSOCIATED CONTENT

Ⓢ Supporting Information

The Supporting Information is available free of charge at https://pubs.acs.org/doi/10.1021/acsomega.1c07084.

> FTIR and Raman spectra for proposed scheme of chemical interactions are shown in S1. Possible mechanism involved in coloration is shown in S2. MS and NMR spectra of as-synthesized colorants are shown in S3−S9 (PDF)

■ AUTHOR INFORMATION

Corresponding Author

> **John H. Xin** − *Institute of Textiles & Clothing, The Hong Kong Polytechnic University, Hong Kong, China; Shenzhen Research Institute, The Hong Kong Polytechnic University, Shenzhen, China*; Email: john.xin@polyu.edu.hk

Authors

> **Suju Fan** − *Institute of Textiles & Clothing, The Hong Kong Polytechnic University, Hong Kong, China; Shenzhen Research Institute, The Hong Kong Polytechnic University, Shenzhen, China;* ⓞ orcid.org/0000-0003-2280-255X
>
> **Yintung Lam** − *Institute of Textiles & Clothing, The Hong Kong Polytechnic University, Hong Kong, China; Shenzhen Research Institute, The Hong Kong Polytechnic University, Shenzhen, China;* ⓞ orcid.org/0000-0002-9293-2950
>
> **Liang He** − *Institute of Textiles & Clothing, The Hong Kong Polytechnic University, Hong Kong, China; Shenzhen Research Institute, The Hong Kong Polytechnic University, Shenzhen, China*

Complete contact information is available at:
https://pubs.acs.org/10.1021/acsomega.1c07084

Notes

The authors declare no competing financial interest.

■ ACKNOWLEDGMENTS

■ REFERENCES

(1) Almeida, M.; Reis, R. L.; Silva, T. H. Marine invertebrates are a source of bioadhesives with biomimetic interest. *Mater. Sci. Eng., C* **2020**, *108*, 110467.

(2) Cai, Z.; Shi, J.; Li, W.; Wu, Y.; Zhang, Y.; Zhang, S.; Jiang, Z. Mussel-inspired pH-switched assembly of capsules with an ultrathin and robust nanoshell. *ACS Appl. Mater. Interfaces* **2019**, *11* (31), 28228−28235.

(3) Silverman, H. G.; Roberto, F. F. Understanding marine mussel adhesion. *Mar. Biotechnol.* **2007**, *9* (6), 661−681.

(4) Ye, Q.; Zhou, F.; Liu, W. Bioinspired catecholic chemistry for surface modification. *Chem. Soc. Rev.* **2011**, *40* (7), 4244−4258.

(5) Fan, C.; Fu, J.; Zhu, W.; Wang, D.-A. A mussel-inspired double-crosslinked tissue adhesive intended for internal medical use. *Acta Biomater.* **2016**, *33*, 51−63.

(6) Cheng, W.; Zeng, X.; Chen, H.; Li, Z.; Zeng, W.; Mei, L.; Zhao, Y. Versatile polydopamine platforms: synthesis and promising applications for surface modification and advanced nanomedicine. *ACS Nano* **2019**, *13* (8), 8537−8565.

(7) Ma, J.; Zhou, T.; Bian, J.; Jie, Y.; Cao, X.; Wang, N. Dopamine polymerization tunes triboelectric interface. *Nano Energy* **2018**, *44*, 199−207.

(8) Bernsmann, F.; Ball, V.; Addiego, F.; Ponche, A.; Michel, M.; Gracio, J. J. d. A.; Toniazzo, V.; Ruch, D. Dopamine-melanin film deposition depends on the used oxidant and buffer solution. *Langmuir* **2011**, *27* (6), 2819−2825.

(9) Lin, J.-H.; Yu, C.-J.; Yang, Y.-C.; Tseng, W.-L. Formation of fluorescent polydopamine dots from hydroxyl radical-induced degradation of polydopamine nanoparticles. *Phys. Chem. Chem. Phys.* **2015**, *17* (23), 15124−15130.

(10) Lee, H.; Dellatore, S. M.; Miller, W. M.; Messersmith, P. B. Mussel-inspired surface chemistry for multifunctional coatings. *Science* **2007**, *318* (5849), 426−430.

(11) Kang, X.; Cai, W.; Zhang, S.; Cui, S. Revealing the formation mechanism of insoluble polydopamine by using a simplified model system. *Polym. Chem.* **2017**, *8* (5), 860−864.

(12) Yuan, Z.; Zhao, Y.; Yang, W.; Hu, Y.; Cai, K.; Liu, P.; Ding, H. Fabrication of antibacterial surface via UV-inducing dopamine polymerization combined with co-deposition Ag nanoparticles. *Mater. Lett.* **2016**, *183*, 85−89.

(13) Gutiérrez-Tauste, D.; Domènech, X.; Domingo, C.; Ayllón, J. A. Dopamine/TiO$_2$ hybrid thin films prepared by the liquid phase deposition method. *Thin Solid Films* **2008**, *516* (12), 3831−3835.

(14) Zhou, R.; Ren, P.-F.; Yang, H.-C.; Xu, Z.-K. Fabrication of antifouling membrane surface by poly(sulfobetaine methacrylate)/polydopamine co-deposition. *Membr. Sci.* **2014**, *466*, 18−25.

(15) Qiu, W.-Z.; Yang, H.-C.; Xu, Z.-K. Dopamine-assisted co-deposition: an emerging and promising strategy for surface modification. *Adv. Colloid Interface Sci.* **2018**, *256*, 111−125.

(16) Zhang, C.; Li, H.-N.; Du, Y.; Ma, M.-Q.; Xu, Z.-K. CuSO$_4$/H$_2$O$_2$-triggered polydopamine/poly(sulfobetaine methacrylate) coatings for antifouling membrane surfaces. *Langmuir* **2017**, *33* (5), 1210−1216.

(17) Hirazawa, H.; Kusamoto, S.; Aono, H.; Naohara, T.; Mori, K.; Hattori, Y.; Maehara, T.; Watanabe, Y. Preparation of fine Mg$_{1-X}$Ca$_X$Fe$_2$O$_4$ powder using reverse coprecipitation method for thermal coagulation therapy in an ac magnetic field. *J. Alloys Compd.* **2008**, *461* (1), 467−473.

(18) Fan, K. W.; Granville, A. M. Surface property modification of silver nanoparticles with dopamine-functionalized poly(pentafluorostyrene) via RAFT polymerization. *Polymers (Basel, Switz.)* **2016**, *8* (3), 81.

(19) Wei, Q.; Wang, X.; Zhou, F. A versatile macro-initiator with dual functional anchoring groups for surface-initiated atom transfer radical polymerization on various substrates. *Polym. Chem.* **2012**, *3* (8), 2129−2137.

(20) Tan, J.; Xie, Z.; Zhang, Z.; Sun, Y.; Shi, W.; Ge, D. Dopamine modified polyaniline with improved adhesion, dispersibility, and biocompatibility. *J. Mater. Sci.* **2018**, *53* (1), 447−455.

(21) Boal, A. K.; Das, K.; Gray, M.; Rotello, V. M. Monolayer exchange chemistry of γ-Fe$_2$O$_3$ nanoparticles. *Chem. Mater.* **2002**, *14* (6), 2628−2636.

(22) Xu, C.; Xu, K.; Gu, H.; Zheng, R.; Liu, H.; Zhang, X.; Guo, Z.; Xu, B. Dopamine as a robust anchor to immobilize functional molecules on the iron oxide shell of magnetic nanoparticles. *J. Am. Chem. Soc.* **2004**, *126* (32), 9938−9939.

(23) Simon, J. D.; Peles, D. N. The red and the black. *Acc. Chem. Res.* **2010**, *43* (11), 1452−1460.

(24) Zou, Y.; Chen, X.; Yang, P.; Liang, G.; Yang, Y.; Gu, Z.; Li, Y. Regulating the absorption spectrum of polydopamine. *Sci. Adv.* **2020**, *6* (36), eabb4696.

(25) Wang, Y.; Su, J.; Li, T.; Ma, P.; Bai, H.; Xie, Y.; Chen, M.; Dong, W. A novel UV-shielding and transparent polymer film: when bioinspired dopamine−melanin hollow nanoparticles join polymers. *ACS Appl. Mater. Interfaces* **2017**, *9* (41), 36281−36289.

(26) Dong, L.; Liu, X.; Xiong, Z.; Sheng, D.; Lin, C.; Zhou, Y.; Yang, Y. Preparation of UV-blocking poly(vinylidene fluoride) films through SI-AGET ATRP using a colorless polydopamine initiator layer. *Ind. Eng. Chem. Res.* **2018**, *57* (38), 12662−12669.

(27) Cheng, K.; Li, M.; Zhang, S.; He, M.; Yu, J.; Feng, Y.; Lu, S. Study on the structure and properties of functionalized fibers with dopamine. *Colloids Surf., A* **2019**, *582*, 123846.

(28) He, L.; Lai So, V. L.; Xin, J. H. Dopamine polymerization-induced surface colouration of various materials. *RSC Adv.* **2014**, *4* (39), 20317−20322.

(29) Lai So, V. L.; He, L.; Xin, J. H. Bio-inspired colouration on various textile materials using a novel catechol colorant. *RSC Adv.* **2014**, *4* (77), 41081−41086.

(30) He, L.; So, V. L. L.; Fan, S.; Xin, J. H. Polyphenol-assisted natural coloration on various synthetic textile materials. *Fibers Polym.* **2018**, *19* (7), 1411−1419.

(31) Willerich, I.; Gröhn, F. Molecular structure encodes nanoscale assemblies: understanding driving forces in electrostatic self-assembly. *J. Am. Chem. Soc.* **2011**, *133* (50), 20341−20356.

(32) Merino, E. Synthesis of azobenzenes: the coloured pieces of molecular materials. *Chem. Soc. Rev.* **2011**, *40* (7), 3835−53.

(33) Ramadan Ali, B.; Ebtissam Jommah, Z.; Khadijah Etohammi, M.; Najjat Omran, I. Synthesis and electric conductivity study of 4-(p-aminophenylazo) benzene sulphonic Acid. *J. Mater. Sci. Eng. B* **2013**.

(34) Haghbeen, K.; Tan, E. W. Facile synthesis of catechol azo dyes. *J. Org. Chem.* **1998**, *63* (13), 4503−4505.

(35) Bohle, D. S.; Rosadiuk, K. A. Nitric oxide catalysis of diazene *E/Z* isomerization. *Inorg. Chem.* **2015**, *54* (15), 7145−51.

(36) Grirrane, A.; Corma, A.; Garcia, H. Preparation of symmetric and asymmetric aromatic azo compounds from aromatic amines or nitro compounds using supported gold catalysts. *Nat. Protoc.* **2010**, *5* (3), 429−438.

(37) Zhang, Z.; Burns, D. C.; Kumita, J. R.; Smart, O. S.; Woolley, G. A. A water-soluble azobenzene cross-linker for photocontrol of peptide conformation. *Bioconjugate Chem.* **2003**, *14* (4), 824−829.

(38) Cai, S.; Rong, H.; Yu, X.; Liu, X.; Wang, D.; He, W.; Li, Y. Room temperature activation of oxygen by monodispersed metal nanoparticles: oxidative dehydrogenative coupling of anilines for azobenzene syntheses. *ACS Catal.* **2013**, *3* (4), 478−486.

(39) Grirrane, A.; Corma, A.; García, H. Gold-catalyzed synthesis of aromatic azo compounds from anilines and nitroaromatics. *Science* **2008**, *322* (5908), 1661.

(40) Kumari, S.; Shekhar, A.; Pathak, D. D. Graphene oxide supported MnO$_2$ nanorods: an efficient heterogeneous catalyst for oxidation of aromatic amines to azo-compounds. *RSC Adv.* **2014**, *4* (105), 61187−61192.

(41) Lekha, L.; Kanmani Raja, K.; Rajagopal, G.; Easwaramoorthy, D. Schiff base complexes of rare earth metal ions: synthesis, characterization and catalytic activity for the oxidation of aniline and substituted anilines. *J. Organomet. Chem.* **2014**, *753*, 72−80.

(42) Zhu, Y.; Shi, Y. Facile Cu(I)-catalyzed oxidative coupling of anilines to azo compounds and hydrazines with diaziridinone under mild conditions. *Org. Lett.* **2013**, *15* (8), 1942−1945.

(43) Lu, L.; He, L.; Zhang, S.; Freeman, H. S. Novel yellow azo-anthraquinone dyes for polylactide fibres: effects of alkyl chain length. *Color. Technol.* **2012**, *128* (2), 121−126.

(44) Ak, M.; Yildiz, H. B.; Toppare, L. Enzyme immobilization in a photosensitive conducting polymer bearing azobenzene in the main chain. *Polym. Bull. (Heidelberg, Ger.)* **2014**, *71* (7), 1827−1841.

(45) Dunetz, J. R.; Magano, J.; Weisenburger, G. A. Large-scale applications of amide coupling reagents for the synthesis of pharmaceuticals. *Org. Process Res. Dev.* **2016**, *20* (2), 140−177.

(46) Hong, D.; Bae, K.; Hong, S.-P.; Park, J. H.; Choi, I. S.; Cho, W. K. Mussel-inspired, perfluorinated polydopamine for self-cleaning coating on various substrates. *Chem. Commun.* **2014**, *50* (79), 11649−11652.

(47) Li, G.; Cheng, G.; Xue, H.; Chen, S.; Zhang, F.; Jiang, S. Ultra low fouling zwitterionic polymers with a biomimetic adhesive group. *Biomaterials* **2008**, *29* (35), 4592−7.

(48) Shi, D.; Shen, J.; Zhao, Z.; Shi, C.; Chen, M. Studies on preparation of poly(3,4-dihydroxyphenylalanine)-polylactide copolymers and the effect of the structure of the copolymers on their properties. *Polymers (Basel, Switz.)* **2016**, *8* (3), 92.

(49) Sundaram, H. S.; Han, X.; Nowinski, A. K.; Ella-Menye, J.-R.; Wimbish, C.; Marek, P.; Senecal, K.; Jiang, S. One-step dip coating of zwitterionic sulfobetaine polymers on hydrophobic and hydrophilic surfaces. *ACS Appl. Mater. Interfaces* **2014**, *6* (9), 6664−6671.

(50) Yang, Y.; Qi, P.; Ding, Y.; Maitz, M. F.; Yang, Z.; Tu, Q.; Xiong, K.; Leng, Y.; Huang, N. A biocompatible and functional adhesive amine-rich coating based on dopamine polymerization. *J. Mater. Chem. B* **2015**, *3* (1), 72−81.

(51) Yang, H.-C.; Xu, W.; Du, Y.; Wu, J.; Xu, Z.-K. Composite free-standing films of polydopamine/polyethyleneimine grown at the air/water interface. *RSC Adv.* **2014**, *4* (85), 45415−45418.

(52) Knorr, D. B.; Tran, N. T.; Gaskell, K. J.; Orlicki, J. A.; Woicik, J. C.; Jaye, C.; Fischer, D. A.; Lenhart, J. L. Synthesis and characterization of aminopropyltriethoxysilane-polydopamine coatings. *Langmuir* **2016**, *32* (17), 4370−4381.

(53) Fan, K. W.; Roberts, J. J.; Martens, P. J.; Stenzel, M. H.; Granville, A. M. Copolymerization of an indazole ligand into the self-polymerization of dopamine for enhanced binding with metal ions. *J. Mater. Chem. B* **2015**, *3* (37), 7457−7465.

(54) Lakshminarayanan, R.; Madhavi, S.; Sim, C. P. C. Oxidative polymerization of dopamine: a high-definition multifunctional coatings for electrospun nanofibers - an overview. *Dopamine - Health and Disease*; IntechOpen: London; United Kingdom, 2018; pp 113−132. DOI: 10.5772/intechopen.81036.

(55) You, I.; Jeon, H.; Lee, K.; Do, M.; Seo, Y. C.; Lee, H. A.; Lee, H. Polydopamine coating in organic solvent for material-independent immobilization of water-insoluble molecules and avoidance of substrate hydrolysis. *J. Ind. Eng. Chem. (Amsterdam, Neth.)* **2017**, *46*, 379−385.

(56) Liu, X.; Kang, J.; Wang, Y.; Li, W.; Guo, H.; Xu, L.; Guo, X.; Zhou, F.; Jia, X. Amine-triggered dopamine polymerization: from aqueous solution to organic solvents. *Macromol. Rapid Commun.* **2018**, *39* (12), 1800160.

(57) Huang, N.; Zhang, S.; Yang, L.; Liu, M.; Li, H.; Zhang, Y.; Yao, S. Multifunctional electrochemical platforms based on the michael addition/schiff base reaction of polydopamine modified reduced graphene oxide: construction and application. *ACS Appl. Mater. Interfaces* **2015**, *7* (32), 17935−17946.

(58) Yang, H.-C.; Luo, J.; Lv, Y.; Shen, P.; Xu, Z.-K. Surface engineering of polymer membranes via mussel-inspired chemistry. *J. Membr. Sci.* **2015**, *483*, 42−59.

(59) Park, J.; Brust, T. F.; Lee, H. J.; Lee, S. C.; Watts, V. J.; Yeo, Y. Polydopamine-based simple and versatile surface modification of polymeric nano drug carriers. *ACS Nano* **2014**, *8* (4), 3347−3356.